

Boundary Noise in Chua's Circuit

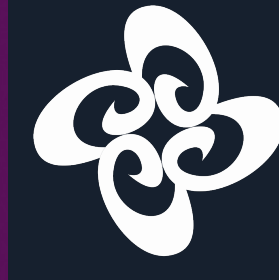
Eoghan J. Staunton

eoghan.staunton@nuigalway.ie

Petri T. Piironen



NUI Galway
OÉ Gaillimh



IRISH RESEARCH COUNCIL
An Chomhairle um Thaighde in Éirinn

1 Introduction

In a smooth dynamical system, given by $\dot{\mathbf{x}} = \mathbf{f}(\mathbf{x})$, the characteristics of a given reference trajectory can be determined by examining the linearised system about the reference trajectory. We can use the *fundamental solution matrix* (FSM) $\phi_{\mathbf{x}}(\mathbf{x}_0^{\text{ref}}, t)$ of the reference trajectory, to approximate the evolution of nearby trajectories. This process is shown in Figure 1.

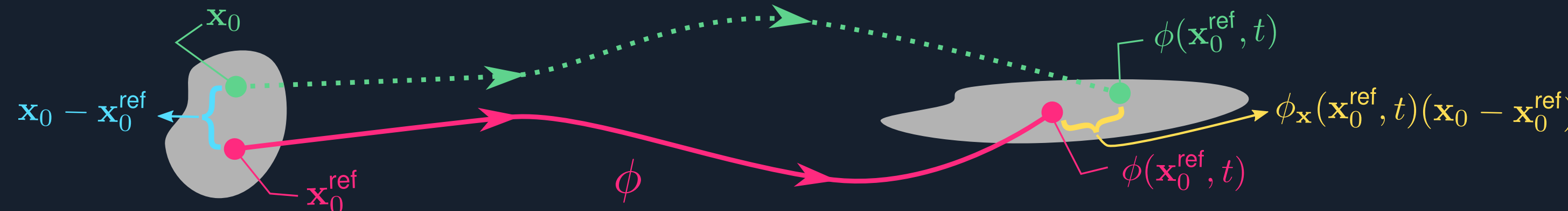


Figure 1
Linearisation of smooth dynamical systems.

This analysis cannot be directly used in nonsmooth systems like the one shown in Figure 2. In nonsmooth systems the vector field \mathbf{f} is not everywhere differentiable, or the flow function $\phi(\mathbf{x}_0^{\text{ref}}, t)$ is not continuous. To account for this we derive the zero-time discontinuity mapping (ZDM) \mathbf{D} , as shown in Figure 3. The Jacobian of \mathbf{D} , evaluated at the crossing point \mathbf{x}_{in} , is called the *saltation matrix*. This matrix allows us to compose the FSMs of the individual flows to give the overall FSM of a crossing trajectory

$$\phi_{\mathbf{x}}(\mathbf{x}_0^{\text{ref}}, T) = \phi_{2,\mathbf{x}}(\mathbf{x}_{\text{out}}, T - t_{\text{ref}}) \mathbf{D}_{\mathbf{x}}(\mathbf{x}_{\text{in}}) \phi_{1,\mathbf{x}}(\mathbf{x}_0^{\text{ref}}, t_{\text{ref}}). \quad (1)$$

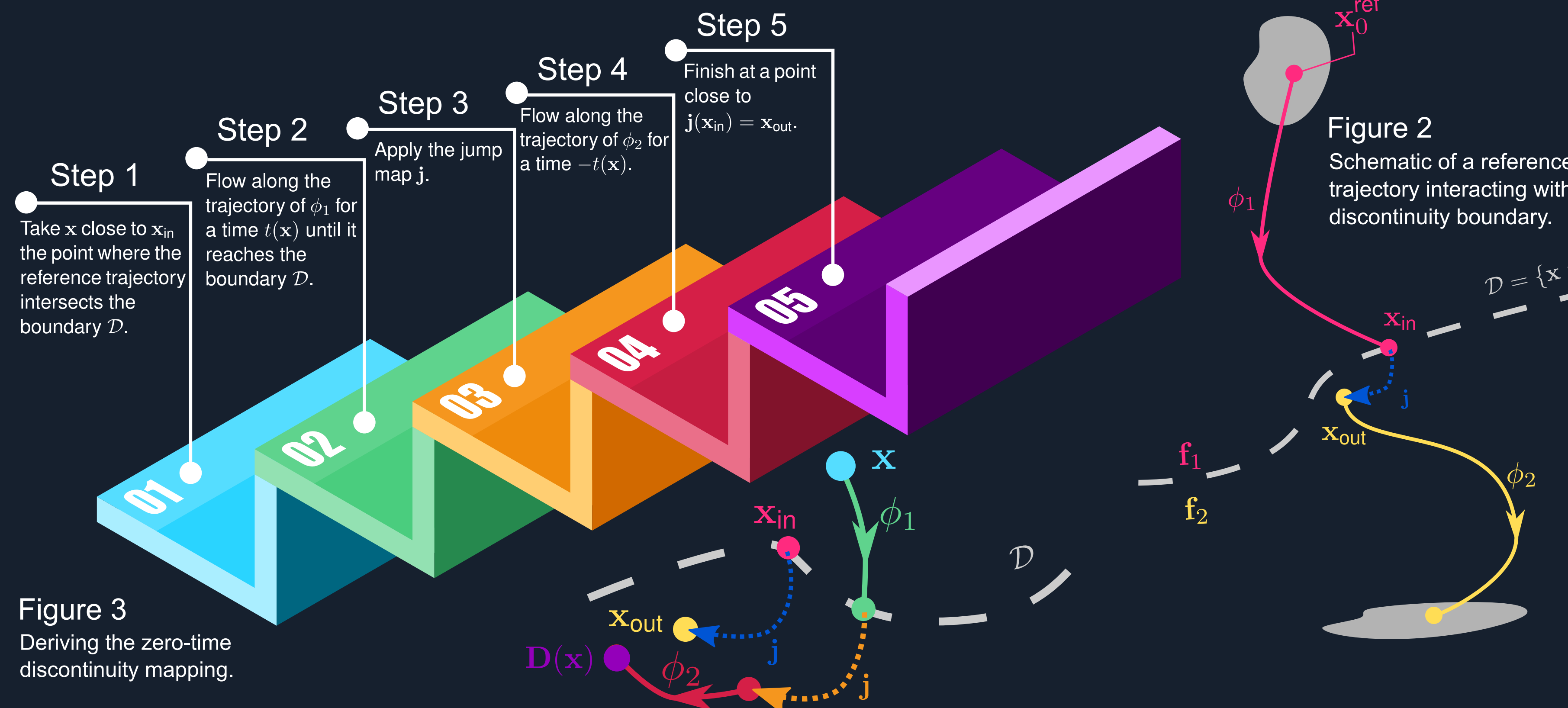


Figure 3
Deriving the zero-time discontinuity mapping.

Our research extends this method to systems which are both nonsmooth and noisy. In particular we consider systems where the position of the discontinuity boundary \mathcal{D} varies randomly in time. Our approach to the problem is as follows:

- First we note that the effect of noise on the reference trajectory can be completely determined by the difference in the time t_{ref} it takes to reach the boundary in the noisy system, compared to \hat{t}_{ref} in the deterministic system.
- We write this difference in time as $\Delta t_{\text{ref}} = t_{\text{ref}} - \hat{t}_{\text{ref}}$ and note that it is a random variable.
- We extend the state space and vector field to $\tilde{\mathbf{x}} = (\mathbf{x}, \Delta t_{\text{ref}}, t)^T$ and $\tilde{\mathbf{f}} = (\mathbf{f}, 0, 1)^T$, respectively.
- We can now think of the realisation of the deterministic reference trajectory in the stochastic system as

$$\tilde{\phi}(\tilde{\mathbf{x}}_0^{\text{ref}}, T) = \tilde{\phi}((\mathbf{x}_0^{\text{ref}}, 0, 0)^T, T) = (\phi(\mathbf{x}_0^{\text{ref}}, T), 0, T)^T. \quad (2)$$

- We then use the approach shown in Figure 3 to derive a stochastic zero-time discontinuity mapping (SZDM) \mathbf{D}^* , allowing us to linearise about the realisation of the deterministic trajectory in the stochastic system.
- Finally, we project back to the original state space \mathbf{x} . Here we find that we can estimate the evolution of deviations from the reference trajectory after time T as

$$\phi(\mathbf{x}_0, T) - \phi(\mathbf{x}_0^{\text{ref}}, T) \approx \phi_{2,\mathbf{x}}(\tilde{\mathbf{x}}_{\text{out}}, T - \hat{t}_{\text{ref}}) \mathbf{D}_{\mathbf{x}}^*(\tilde{\mathbf{x}}_{\text{in}}) \phi_{1,\mathbf{x}}(\tilde{\mathbf{x}}_{\text{in}}, \hat{t}_{\text{ref}}) (\mathbf{x}_0 - \tilde{\mathbf{x}}_0^{\text{ref}}) + \phi_{2,\mathbf{x}}(\tilde{\mathbf{x}}_{\text{out}}, T - \hat{t}_{\text{ref}}) (\hat{\mathbf{f}}_{\text{in}} - \hat{\mathbf{f}}_{\text{out}}) \Delta t_{\text{ref}}, \quad (3)$$

where $\tilde{\mathbf{x}}_{\text{in}}$, $\tilde{\mathbf{x}}_{\text{out}}$, $\hat{\mathbf{f}}_{\text{in}}$, $\hat{\mathbf{f}}_{\text{out}}$, \hat{t}_{ref} are the values associated with the reference trajectory in the deterministic system and $\mathbf{D}_{\mathbf{x}}^*(\tilde{\mathbf{x}}_{\text{in}})$ is the Jacobian derivative of the SZDM evaluated at the deterministic crossing point.

Suppose now we want to define a map \mathbf{M} that describes the distribution about a periodic trajectory that crosses N noisy boundaries with switches so that

$$\mathbf{x}_{k+1} = \mathbf{M}(\mathbf{x}_k), \quad k = 0, 1, \dots \quad (4)$$

This can be done if we let the map \mathbf{M} be defined as

$$\mathbf{M}(\mathbf{x}) = \phi_{N,\mathbf{x}} \mathbf{K}_N(\mathbf{x}), \quad (5)$$

where

$$\mathbf{K}_0(\mathbf{x}) = \mathbf{x}, \quad \text{and} \quad \mathbf{K}_n(\mathbf{x}) = \mathbf{D}_{n,\mathbf{x}}^* \phi_{n,\mathbf{x}} \mathbf{K}_{n-1}(\mathbf{x}) + (\hat{\mathbf{f}}_n^{\text{in}} - \hat{\mathbf{f}}_n^{\text{out}}) \Delta t_n, \quad \text{for } n \geq 1. \quad (6)$$

References

1. M. di Bernardo, C. Budd, A.R. Champneys, and P. Kowalczyk, *Piecewise-smooth dynamical systems: theory and applications*, vol. 163, Springer, 2008.
2. L.O. Chua, M. Komuro, and T. Matsumoto, The double scroll family, *IEEE transactions on circuits and systems*, 33(11):1072-1118, 1986.
3. E.J. Staunton and P.T. Piironen, Estimating the Dynamics of Systems with Noisy Boundaries, *In Preparation*, 2019.

2 Chua's Circuit

Chua's circuit is a nonlinear circuit that was created with the aim of being the simplest autonomous circuit capable of generating chaos. It was the first physical system for which the presence of chaos was shown experimentally, numerically and mathematically. The circuit, shown in Figure 5, contains four linear elements and one nonlinear resistor known as a *Chua's diode*. The piecewise-linear V - I characteristic of Chua's diode is shown in Figure 6. The circuit can be easily and cheaply constructed using standard electronic components. Chua's circuit can be described by the following nondimensionalised state equations

$$\begin{aligned} \dot{x} &= \alpha(y - x - g(x)), \\ \dot{y} &= x - y + z, \\ \dot{z} &= -(\beta y + \gamma z), \end{aligned} \quad (7)$$

where $g(x)$ is the piecewise linear function representing the V - I characteristic of Chua's diode

$$g(x) = \begin{cases} m_1 x + m_1 - m_0 & \text{if } x < -1, \\ (m_0 - \epsilon)x & \text{if } |x| \leq 1, \\ m_1 x + m_0 - m_1 & \text{if } x > 1. \end{cases} \quad (8)$$

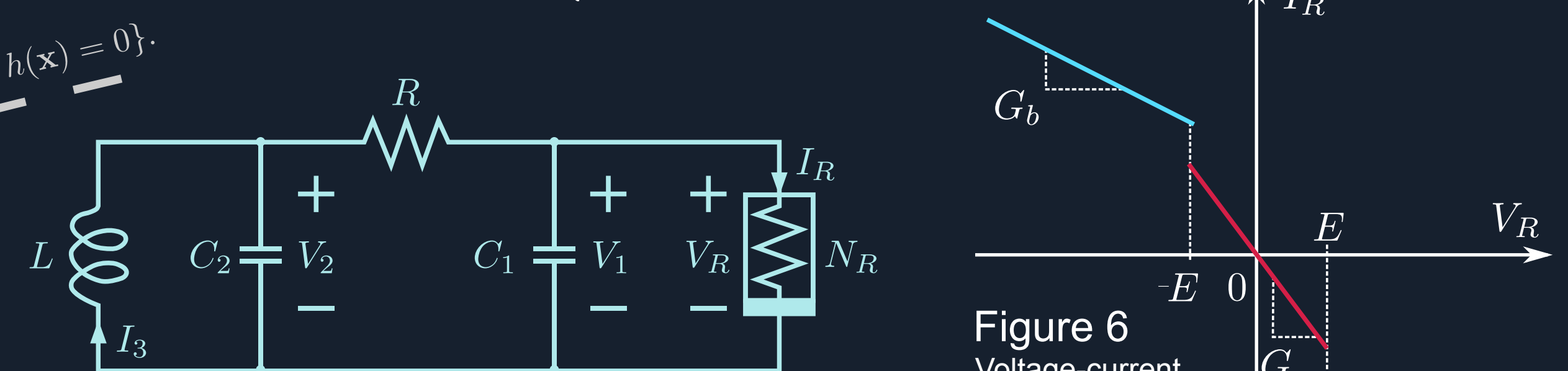


Figure 5
Chua's circuit including Chua's diode N_R .

Figure 6
Voltage-current characteristic of Chua's diode.

3 Attractors in Chua's Circuit

Despite its simplicity Chua's circuit displays a huge variety of complex behaviours. In previous studies a wide range of periodic, quasiperiodic, strange and chaotic attractors have been found and both the period-doubling and intermittency routes to chaos have been observed. A selection of Chua attractors are shown in Figure 7. Here we focus on estimating the effects of boundary noise on periodic *hidden attractors* in Chua's circuit. Unlike most classical attractors which are *self-excited*, there are no transient processes leading to hidden attractors from neighborhoods of unstable equilibria. As a result they can be difficult to find and to visualise.

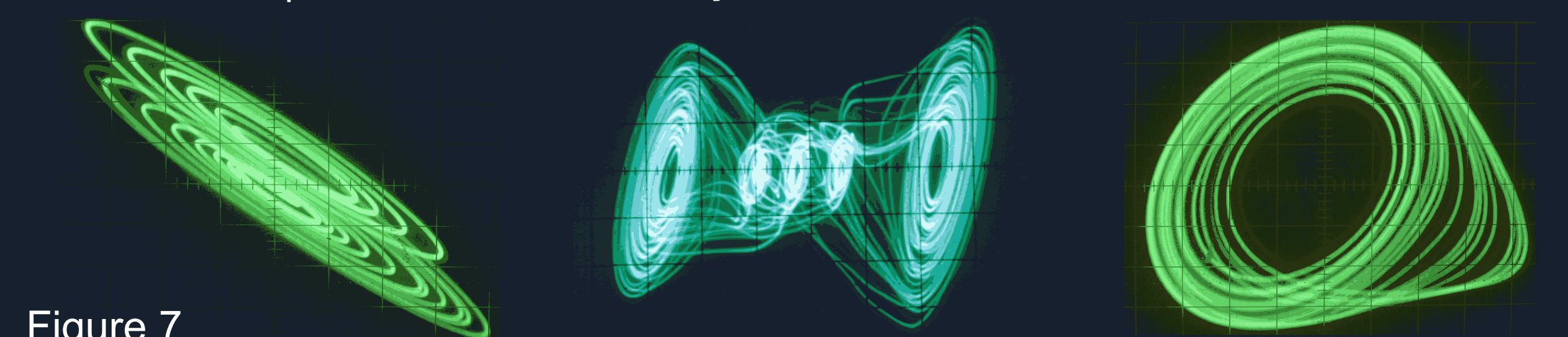


Figure 7
Gallery of attractors that appear in Chua's circuit.

In particular, for appropriate parameter values the system (7) has five coexisting attractors which are plotted in Figure 8. These include two equilibrium points ($\mathbf{x}_{\text{eq}}^{\pm}$), two small symmetric hidden periodic attractors (C^{\pm}) and one large periodic attractor (C^{∞}). The intersection of their basins of attraction with the boundary at $x = -1$ is shown in Figure 9. We will examine the effects of noise on the small symmetric hidden periodic attractors C^{\pm} by using the methods detailed in the Introduction.

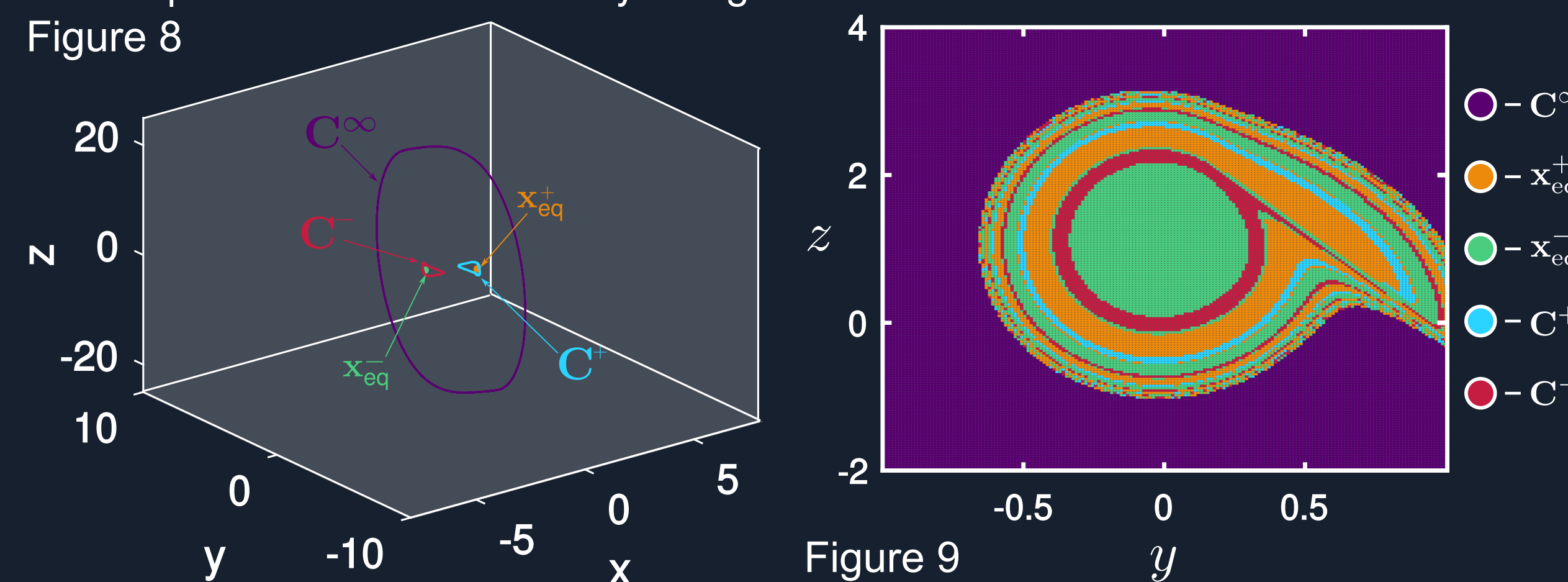
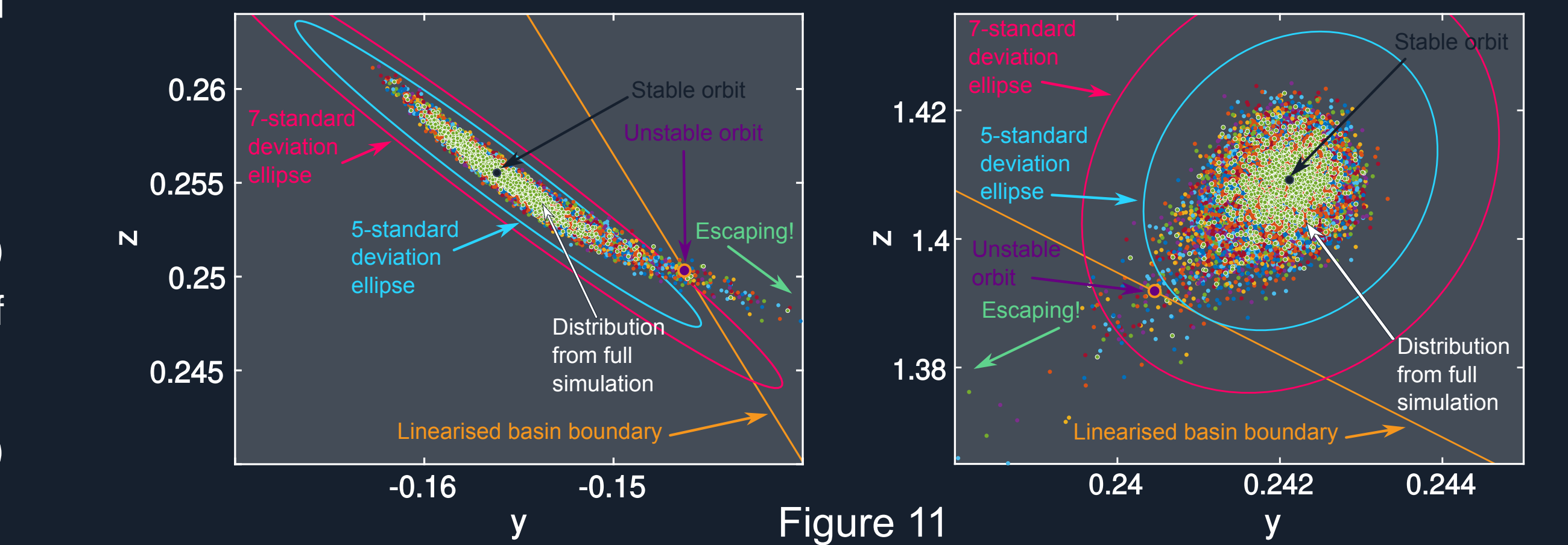


Figure 8

Figure 9

4 Important Deterministic Features

- We now introduce some important features of (7) in the 5-stable regime (Figure 8).
1. The symmetric periodic orbits C^{\pm} are destroyed in saddle bifurcations if the magnitude of the discontinuity parameter ϵ becomes too large.
 2. There C^{\pm} collide with corresponding unstable periodic orbits C_u^{\pm} .
 3. The stable manifolds of C_u^{\pm} form the closest boundaries of the basins of attraction of C^{\pm} , respectively.
 4. Intersections of the stable manifolds of C_u^{\pm} with $x = \pm 1$ can be linearly estimated by the eigenvectors of the associated Poincaré mappings.

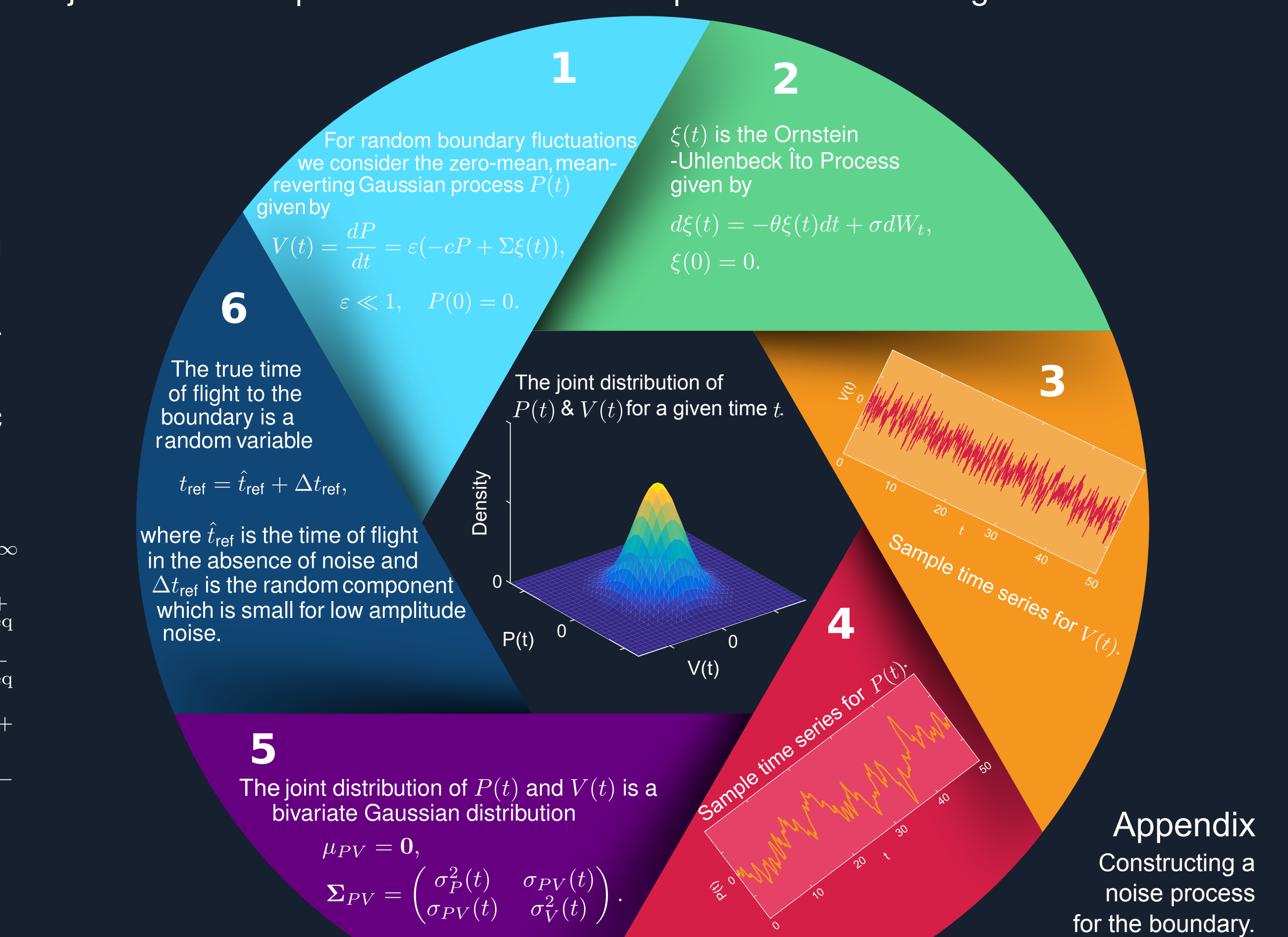


5 Estimating the Effects of Noise

Here we will estimate the amplitude of noise required to push trajectories out of periodic behaviour. Our approach is as follows. We:

1. Construct maps $\delta_n^i = \mathbf{M}_i(\delta_{n-1}^i)$ which give the distribution of errors δ_n^i , about starting points \mathbf{x}^i on C^i , after n periods. (Following the schematic in Figure 4.)
2. Choose our two starting points to be the two intersections of C^- with the discontinuity boundary at $x = -1$, with starting errors $\delta_0^i = 0$.
3. Project the resulting trivariate distributions onto the discontinuity boundary where they become bivariate distributions in the (y, z) -plane.
4. Find that the distributions converge to invariant distributions.
5. Compare the invariant distributions to the system's deterministic features.

In particular, we consider how invariant distributions interact with the system's basins of attraction. We note trajectories can only escape basins when crossing a noisy boundary. Elsewhere, the system's evolution is deterministic. Thus it is sufficient to consider the distributions on the deterministic discontinuity boundary as described above. We construct N -standard-deviation ellipses using the eigenvalues and vectors of the linearised distribution's covariance matrix. If an ellipse crosses the basin boundary it indicates a probability that trajectories will be pushed out of periodic behaviour by noise. On the other hand, if the ellipse is contained within the periodic orbit's basin for high N it indicates that the noise level is not sufficiently high to push trajectories out of periodic behaviour. Examples are shown in Figures 10 and 11.



Appendix
Constructing a noise process for the boundary.